The Effect of Cyclization of Magainin 2 and Melittin Analogues on Structure, Function, and Model Membrane Interactions: Implication to Their Mode of Action

Tamar Unger,[‡] Ziv Oren,[‡] and Yechiel Shai*[,§]

Department of Biological Chemistry, The Weizmann Institute of Science, Rehovot, 76100 Israel

Received November 13, 2000; Revised Manuscript Received February 12, 2001

ABSTRACT: The amphipathic α-helical structure is a common motif found in membrane binding polypeptides including cell lytic peptides, antimicrobial peptides, hormones, and signal sequences. Numerous studies have been undertaken to understand the driving forces for partitioning of amphipathic α-helical peptides into membranes, many of them based on the antimicrobial peptide magainin 2 and the non-cell-selective cytolytic peptide melittin, as paradigms. These studies emphasized the role of linearity in their mode of action. Here we synthesized and compared the structure, biological function, and interaction with model membranes of linear and cyclic analogues of these peptides. Cyclization altered the binding of melittin and magainin analogues to phospholipid membranes. However, at similar bound peptide:lipid molar ratios, both linear and cyclic analogues preserved their high potency to permeate membranes. Furthermore, the cyclic analogues preserved ∼75% of the helical structure of the linear peptides when bound to membranes. Biological activity studies revealed that the cyclic melittin analogue had increased antibacterial activity but decreased hemolytic activity, whereas the cyclic magainin 2 analogue had a marked decrease in both antibacterial and hemolytic activities. The results indicate that the linearity of the peptides is not essential for the disruption of the target phospholipid membrane, but rather provides the means to reach it. In addition, interfering with the coil−helix transition by cyclization, while maintaining the same sequence of hydrophobic and positively charged amino acids, allows a separated evaluation of the hydrophobic and electrostatic contributions to binding of peptides to membranes.

Binding of membrane-active polypeptides such as viral fusion peptides, hormones, signal sequences, and cytolytic peptides depends less on the actual amino acid composition but rather on global structural properties such as peptide charge, hydrophobicity, and helicity (*1*, *2*). Numerous studies have been undertaken to determine the nature of interaction of the cytolytic peptides melittin, the major component of honey bee (*Apis mellifera)* venom (*3*), and magainin 2, isolated from the skin of the African clawed frog (*Xenopus laevis*) (*4*), as paradigms for studying the driving forces responsible for partitioning amphipathic α-helical peptides into membranes. These peptides have similar charge, structure, and organization within the membrane. Melittin is a 26 amino acid peptide with a high (+6) positive charge. In aqueous solutions, the monomer has no detectable secondary structure (*5*, *6*). Membrane-bound melittin consists of two α-helical segments (residues 2−10 and 13−21) (*7*−*10*). The helices are connected by a hinge (*11*, *12*) forming a bent α-helical rod where the hydrophilic and hydrophobic sides face in opposite directions. Charged residues are mainly located at the C-terminus. Spin-label EPR and ATR-FTIR results indicate melittin bound to fully hydrated bilayers is located at the interface with both helices oriented approximately parallel to the plane of the membrane (*11*−*13*). Magainin 2 is a 23 amino acid antimicrobial peptide, also highly basic (+5) but with more dispersed charged residues. In aqueous solutions, magainin 2 is unstructured (*14*). In the presence of sodium dodecyl sulfate micelles (SDS) or lipid vesicles, magainin 2 exists mainly in an α-helical conformation (*15*−*17*). In contrast to melittin, magainin 2 does not contain a proline residue. However, two-dimensional ^{1}H NMR experiments show that the membrane-bound state of magainin is curved, with a bend centered at residues Phe^{12} and Gly^{13} (*18*), and is oriented parallel to the membrane surface (*19*−*22*).

Despite similarities in structure and organization within the membrane, melittin and magainin 2 display significant differences in cell selectivity. Both peptides possess high antibacterial activity against Gram-positive and Gram-negative bacteria (*4*, *23*, *24*); however, melittin is significantly more hemolytic (*25*, *26*). Melittin's lack of cell selectivity arises from nonspecific interactions with zwitterionic (major component of normal mammalian cell) and negatively charged (major component of bacterial membrane) membranes (*27*−*32*), whereas magainin 2 preferentially binds negatively charged phospholipids (*16*, *21*, *33*, *34*).

Several distinct hypotheses were proposed to explain the mechanism of membrane lysis by melittin (*35*−*37*) and magainin 2 (*38*, *39*). Further studies support the hypothesis that both melittin and magainin lyse membranes by inter-

* To whom correspondence should be addressed at the Department of Biological Chemistry, The Weizmann Institute of Science, Rehovot, 76100 Israel. Tel: 972-8-9342711; Fax: 972-8-9344112; Email: Yechiel.Shai@weizmann.ac.il.

‡ These authors contributed equally to the study.

§ Recipient of The Harold S. and Harriet B. Brady Professorial Chair in Cancer Research.

10.1021/bi0026066 CCC: $20.00
Published on Web 05/03/2001

calating within the lipid interface and acyl chain region and disrupting the lipid order, as opposed to forming transmembrane pores [for reviews, see (*40*−*42*)]. These studies emphasized the importance of amphipathicity and α-helicity to the cytolytic activity of the peptides. An additional attribute, common among native amphipathic helices including melittin and magainin, is peptide linearity. To our knowledge, the role of linearity in biological function and mode of action has not yet been examined. For this purpose, we synthesized linear and cyclic analogues of melittin and magainin 2 and characterized the biological activity of these peptides toward erythrocytes and bacteria, as well as their interaction with model phospholipid membranes. The peptide secondary structures when bound to zwitterionic or net negatively charged phospholipid membranes were determined by circular dichroism (CD)[1] spectroscopy. These cyclic analogues offer unique insight into the mode of peptide interactions with membranes and provide important information on parameters that affect cell selectivity.

MATERIALS AND METHODS

Materials. Rink amide 4-methyl benzhydrylamine resin (MBHA) and fluoren-9-ylmethoxycarbonyl (Fmoc) amino acids were purchased from Calibochem−Novabiochem (La Jolla, CA). Other reagents used for peptide synthesis included trifluoroacetic acid (TFA, Sigma), methylene chloride (peptide synthesis grade, Biolab, IL), dimethylformamide (peptide synthesis grade, Biolab), piperidine (Merck, Darmstadt, Germany), and benzotriazolyl-*N*-oxytris(dimethylamino)-phosphonium hexafluorophosphate (BOP, Sigma). Egg phosphatidylcholine (PC), egg phosphatidylglycerol (PG), phosphatidylethanolamine (PE) (type V, from *Escherichia coli*), L-α-lysophosphatidylcholine (LPC) (type I, from egg yolk), methyl methanethiosulfonate (MMTS), and 4-fluoro-7-nitrobenz-2-oxa-1,3-diazole (NBD-F) were purchased from Sigma. 3,3′-Diethylthiodicarbocyanine iodide (diS-C_2-5) was obtained from Molecular Probes (Eugene, OR). Cholesterol (extra pure) was supplied by Merck (Darmstadt, Germany) and recrystallized twice from ethanol. All other reagents were of analytical grade. Buffers were prepared in double glass-distilled water.

Peptide Synthesis, Fluorescent Labeling, and Purification. Peptides were synthesized by solid-phase methods using standard fluoren-9-ylmethoxycarbonyl (Fmoc) chemistry on Rink amide MBHA resin. The peptides were synthesized with cysteine residues at both their N- and C-termini. Labeling of the N-terminus of the peptides with the fluorescent probe 7-nitrobenz-2-oxa-1,3-diazole (NBD) was achieved by labeling the resin-bound peptide as described previously (*43*). The peptides were cleaved from the resins by trifluoroacetic acid (TFA) and purified by RP-HPLC on a C_{18} reverse-phase Bio-Rad semi-preperative column (250 × 10 mm, 300 Å pore size, 5 μm particle size). The column was eluted in 40 min, using a linear gradient of 10−60% acetonitrile in water, both containing 0.05% TFA (v/v), at a flow rate of 1.8 mL/min. Purified peptides were solubilized at a concentration of 35 mg/L in sodium acetate (pH 7.3), and were allowed to form a disulfide bond by air oxidation for 24 h, at room temperature under stirring. The cyclic peptides were further purified by RP-HPLC and were shown to be homogeneous (∼95%). To obtain linear peptides, the free cysteine-containing peptides were treated with methyl methanethiosulfonate (MMTS). The peptides were subjected to amino acid analysis and electrospray mass spectroscopy to confirm their composition and molecular weight.

Preparation of Liposomes. Small unilamellar vesicles (SUV) were prepared by sonication of PC/cholesterol (10:1 w/w) or PE/PG (7:3 w/w) dispersions as described in detail previously (*43*). Large unilamellar vesicles (LUV) were also prepared from PC/PG (7:3 w/w) as follows: dry lipids were suspended in PBS buffer by vortexing to produce large multilamellar vesicles. The lipid suspension was freeze−thawed 6 times and then extruded 20 times through polycarbonate membranes with 0.1 m diameter pores (Nuclepore Corp., Pleasanton, CA). Vesicles were visualized using a JEOL JEM 100B electron microscope (Japan Electron Optics Laboratory Co., Tokyo, Japan) as follows. A drop of vesicles was deposited on a carbon-coated grid and negatively stained with uranyl acetate. Examination of the grids demonstrated that the vesicles were unilamellar with an average diameter of 20−50 nm for SUV (*44*) or 100 nm for LUV.

Antibacterial Activity of the Peptides. The antibacterial activity of the peptides was examined in sterile 96-well plates (Nunc F96 microtiter plates) in a final volume of 100 μL as follows. Aliquots (50 μL) of a bacterial suspension at a concentration of 10^6 colony-forming units (CFU)/mL in culture medium (LB medium) were added to 50 μL of aqueous peptide solution created by serial 2-fold dilutions in water. Inhibition of bacterial growth was determined by measuring the absorbance at 600 nm with a Microplate autoreader El309 (Bio-Tek Instruments) after an incubation of 18−20 h at 37 °C. Antibacterial activities are expressed as the minimal inhibitory concentration (MIC), the concentration at which 100% inhibition of growth occurred after 18−20 h of incubation. The bacteria used were: *Escherichia coli* D21, *Acinetobacter calcoaceticus* Ac11, *Micrococcus luteus* ATCC 9341, and *Bacillus subtilis* ATCC 6051.

Hemolysis of Human Red Blood Cells (hRBC). Fresh hRBC with EDTA were rinsed 3 times with PBS (35 mM phosphate buffer/0.15 M NaCl, pH 7.3) by centrifugation for 10 min at 800*g* and resuspended in PBS. Peptides dissolved in PBS were then added to 50 μL of a solution of the stock hRBC in PBS to reach a final volume of 100 μL (final erythrocyte concentration, 4% v/v). The resulting suspension was incubated under agitation for 60 min at 37 °C. The samples were then centrifuged at 800*g* for 10 min. Release of hemoglobin was monitored by measuring the absorbance of the supernatant at 540 nm. Controls for zero hemolysis (blank) and 100% hemolysis consisted of hRBC suspended in PBS and Triton 1%, respectively.

Membrane Permeation Induced by the Peptides. Membrane destabilization, which results in the collapse of a diffusion potential, was detected fluorometrically as previ-

[1] Abbreviations: BHA, 4-methyl benzhydrylamine resin; CD, circular dichroism; CFU, colony-forming units; diS-C_2-5, 3,3′-diethylthiodicarbocyanine iodode; Fmoc, fluoren-9-ylmethoxycarbonyl; HEPES, *N*-(2-hydroxyethyl)piperazine-*N*′-2-ethanesulfonic acid; hRBC, human red blood cells; LPC, lysophosphatidylcholine; MIC, minimal inhibitory concentration; MMTS, methyl methanethiosulfonate; NBD-F, 4-fluoro-7-nitrobenz-2-oxa-1,3-diazole; PBS, phosphate-buffered saline; PC, egg phosphatidylcholine; PE, *E. coli* phosphatidylethanolamine; PG, egg phosphatidylglycerol; RP-HPLC, reverse-phase high-performance liquid chromatography; SUV, small unilamellar vesicles; TFA, trifluoroacetic acid.

Table 1: Sequences and Designations of the Peptides Investigated

Peptide Designation	Sequence [a,b]
Linear melittin analog	CH_3-S- C G I G A V L K V L T T G L P A L I S W I K R K R Q Q C-S-CH_3
Cyclic melittin analog	C G I G A V L K V L T T G L P A L I S W I K R K R Q Q C
Linear magainin 2 analog	CH_3-S- C G I G K F L H S A K K W G K A F V G A I M N S C-S-CH_3
Cyclic magainin 2 analog	C G I G K F L H S A K K W G K A F V G A I M N S C

[a] The C-terminal is amidated. [b] CH_3-S is bound to Cys.

ously described (*45*−*47*). Briefly, a liposome suspension, prepared in "K^+ buffer" (50 mM K_2SO_4/25 mM HEPES-sulfate, pH 6.8), was added to an isotonic K^+-free buffer (50 mM Na_2SO_4/25 mM HEPES-sulfate, pH 6.8), and the dye diS-C_2-5 was then added. Subsequent addition of valinomycin created a negative diffusion potential inside the vesicles by a selective afflux of K^+ ions, which resulted in a quenching of the dye's fluorescence. Peptide-induced membrane permeation for all the ions in the solution caused a dissipation of the diffusion potential, as monitored by an increase in fluorescence. Fluorescence was monitored using excitation and emission wavelengths at 620 and 670 nm, respectively. The percentage of fluorescence recovery, F_t, was defined by

$$F_t = [(I_t - I_o)/(I_f - I_o)] \times 100$$

where I_t = fluorescence observed after addition of a peptide at time t, I_o = fluorescence after addition of valinomycin, and I_f = total fluorescence prior to the addition of valinomycin.

Binding of Peptides to Vesicles. The affinity of the peptides to phospholipid membranes was evaluated using NBD-labeled peptides. NBD fluorescence is sensitive to the polarity of the environment; therefore, the fluorescence of an NBD-labeled peptide increases upon transfer from a solution to a hydrophobic environment. The degree of peptide association with zwitterionic [PC/cholesterol (10:1 w/w)] or net negatively charged phospholipids [PE/PG (7:3 w/w) or PC/PG (7:3 w/w)] was measured by adding 0.1 μM NBD-labeled peptide to 2 mL of PBS solution in the presence of SUV at different concentrations. The fluorescence intensity was measured in the time-dependent mode, with excitation set at 467 nm, emission set at 530 nm, and slits set to 8 nm, until a maximal intensity was achieved. Measurements were taken at several vesicle concentrations. The fluorescence values, F, were corrected by subtracting the corresponding blank (buffer with the same amount of vesicles). The increases in the fluorescence intensity, $F - F_0$, where F_0 is the fluorescence intensity in the absence of vesicles, were plotted as a function of the lipid:peptide molar ratio.

The partition coefficient was determined by nonlinear least-squares (NLLSQ) fitting using the equations:

$$f = f_{bound} f_{max} + (1 - f_{bound}) f_0$$

$$f_{bound} = K_p L/(W + K_p L)$$

where W is the water concentration (55.56 M) and L is the molar lipid concentration. NLLSQ analyses and data simulations were performed with the commercial software package Origin 6.0 (MicroCal, Inc., Northampton, MA).

CD Spectroscopy. The CD spectra of the peptides were measured with a Jasco J-500A spectropolarimeter after calibrating the instrument with (+)-10-camphorsulfonic acid. The spectra were scanned at 25 °C in a capped, quartz optical cell with a 0.5 mm path length. Spectra were obtained at wavelengths of 250−190 nm. Eight scans were taken for each peptide at a scan rate of 20 nm/min. The peptides were scanned at concentrations of 1.5×10^{-5} to 2.0×10^{-5} M in PBS (35 mM phosphate buffer/0.15 M NaCl, pH 7.3) and in the presence of PE/PG (7:3, w/w, 6.5 mM final concentration) SUV or 2% lysophosphatidylcholine (LPC) micelles. Fractional helicities (*48*, *49*) were calculated as

$$\frac{[\theta]_{222} - [\theta]^0_{222}}{[\theta]^{100}_{222} - [\theta]^0_{222}}$$

where $[\theta]_{222}$ is the experimentally observed mean residue ellipticity at 222 nm, and the values for $[\theta]^0_{222}$ and $[\theta]^{100}_{222}$, which correspond to 0% and 100% helix content at 222 nm, are estimated to be 2000 and 32 000 deg·cm^2/dmol, respectively (*49*).

RESULTS

The amino acid sequences of the peptides are presented in Table 1. An analogue of magainin 2 was used, in which Phe 12 was replaced by Trp and Glu 19 was replaced by Ala. In addition, both peptides were synthesized with cysteines at their N- and C-termini. Functional and structural studies revealed that the Phe 12 to Trp substitution did not change the properties of the parent peptide (*22*, *50*). The Glu 19 to Ala substitution resulted in significantly increased antimicrobial activity (*20*, *51*). The resulting $W_{12}A_{19}$-magainin 2 (magainin 2 analogue) has a net positive charge of +6 and the same intrinsic fluorescent probe (Trp) as melittin. Cyclic analogues of melittin and magainin 2 were prepared by forming a disulfide bond between two Cys residues. The linear peptides were prepared by blocking the reduced cysteines with methyl methanethiosulfonate (MMTS), a cysteine-specific reagent. As expected, mass spectrometry revealed molecular weights of 3142 for linear melittin, 3048 for cyclic melittin, 2743 for linear magainin 2 analogue, and 2649 for cyclic magainin 2 analogue. All assays were also

Table 2: Minimal Inhibitory Concentration (μM) of the Peptides[a]

peptide designation	minimal inhibitory concentration			
	E. coli (D21)	*A. calcoaceticus* (AC11)	*M. luteus* (ATCC 9341)	*B. subtilis* (ATCC 6051)
linear melittin analogue	32	4	2	2
cyclic melittin analogue	10	3	1.5	0.8
linear magainin 2 analogue	4	2.5	2.5	2
cyclic magainin 2 analogue	>100	19	80	11
tetracycline	1.5	1.5	0.5	6.5

[a] Results are the mean of 3 independent experiments each performed in duplicate, with the standard deviation not exceeding 25%.

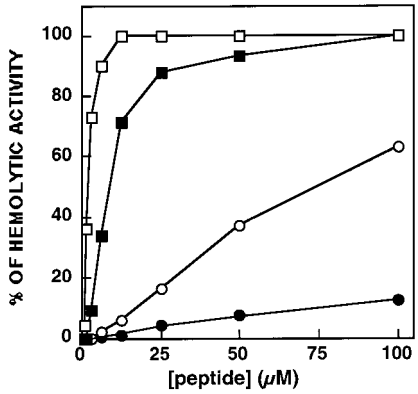

FIGURE 1: Dose−response of the hemolytic activity of the peptides toward hRBC. The assay was performed as described under Materials and Methods. Designations are as follows: linear melittin (□); cyclic melittin (■); linear magainin 2 analogue (○); cyclic magainin 2 analogue (●).

performed with the NBD-labeled peptides, and the results were nearly identical to those obtained with unlabeled peptides, as has been shown also in other studies (*52*, *53*).

Antimicrobial and Hemolytic Activities of the Peptides. Antibacterial activity was assayed against a representative set of test bacteria including both Gram-negative species (*Escherichia coli* and *Acinetobacter calcoaceticus*) and Gram-positive species (*Bacillus subtilis* and *Micrococcus luteus*). The antibiotic tetracycline served as a control. The results of this study are summarized in Table 2. The cyclization of melittin increases its activity against all bacteria examined, most significantly toward *E. coli*. In contrast, cyclization of magainin 2 analogue markedly decreases its antibacterial activity against both Gram-positive and Gram-negative bacteria.

The peptides were also tested for their hemolytic activity against the highly sensitive human erythrocytes. A dose−response curve of peptide hemolytic activity (Figure 1) shows that peptide cyclization substantially decreases the hemolytic activity of both melittin and magainin 2 analogue.

Binding Studies. Two possible mechanisms may explain the reduced hemolytic activity of the cyclic peptides. They may bind with lower affinity to different phospholipid membranes, or once bound may not be able to organize into structures that induce membrane lysis. The single tryptophan was used as an intrinsic fluorescence probe to follow peptide binding to model phospholipid membranes. Only small increases in the fluorescence intensity were observed upon titration of both cyclic and linear peptides. A possible

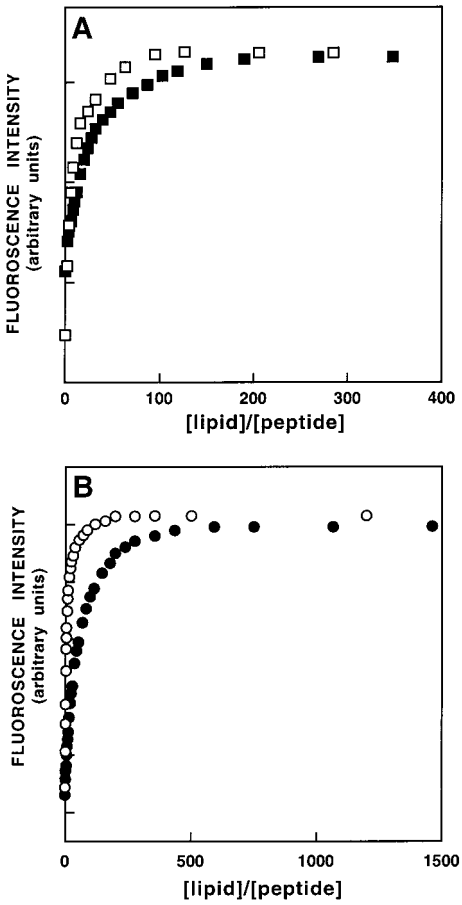

FIGURE 2: Panel A: Increases in the fluorescence of NBD-labeled linear melittin (□) and cyclic melittin (■) (0.1 μM total concentration) upon titration with PE/PG vesicles, with the excitation wavelength set at 467 nm and emission at 530 nm. The experiment was performed at 25 °C in PBS. Panel B: Increases in the fluorescence of NBD-labeled linear magainin 2 analogue (○) and cyclic magainin 2 analogue (●) (0.1 μM total concentration) upon titration with PE/PG vesicles.

explanation is that conformational changes occur when peptides bind vesicles that place the tryptophan residue in the vicinity of the disulfide bond, a quencher of Trp fluorescence (*54*, *55*). Therefore, the peptides were labeled at the N-terminus with the fluorophore NBD, which is highly sensitive to the dielectric constant of its environment. A fixed concentration (0.1 μM) of peptide was titrated with vesicles [either net negatively charged PE/PG vesicles (7:3 w/w), a phospholipid composition typical of *E. coli* (*56*), or zwitterionic PC/cholesterol (10:1, w/w) vesicles, a phospholipid composition used to mimic the major components of the outer leaflet of human erythrocytes (*57*)], while monitoring the increase in fluorescence caused by binding. LUV composed of net negatively charged PC/PG (7:3 w/w) were also used as a control. Plotting the increase in NBD fluorescence as a function of lipid:peptide molar ratios yielded conventional binding curves (Figures 2−4).

The results, summarized in Table 3, reveal a relatively small increase (~4-fold higher) in the affinity of the linear melittin analogue to PE/PG and PC/PG versus the cyclic form. In comparison, a larger increase (~10-fold) occurred with magainin analogues. When the peptides bind PC/cholesterol vesicles, the differences in affinity increase to 30-fold and ~70-fold between the linear and the cyclic forms for melittin and magainin 2 analogues, respectively. To verify

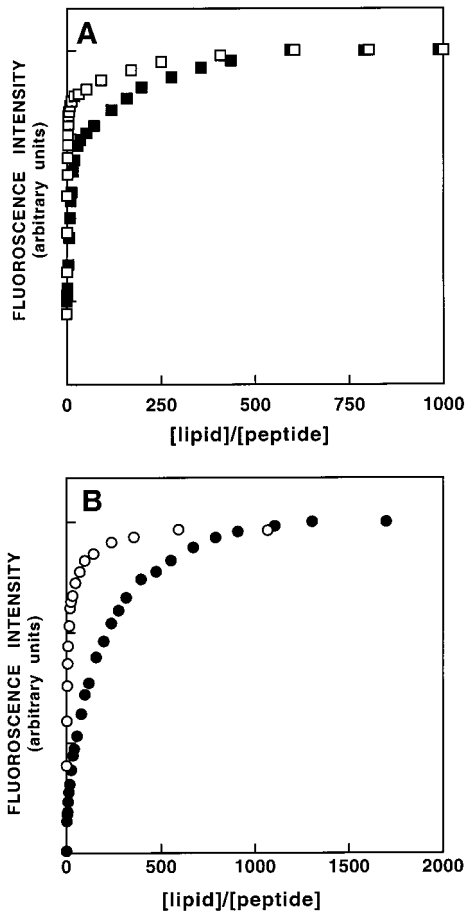

FIGURE 3: Panel A: Increases in the fluorescence of NBD-labeled linear melittin (□) and cyclic melittin (■) (0.1 μM total concentration) upon titration with PC/PG vesicles, with the excitation wavelength set at 467 nm and emission at 530 nm. Details are as depicted in the legend to Figure 2. Panel B: Increases in the fluorescence of NBD-labeled linear magainin 2 analogue (○) and cyclic magainin 2 analogue (●) (0.1 μM total concentration) upon titration with PC/PG vesicles.

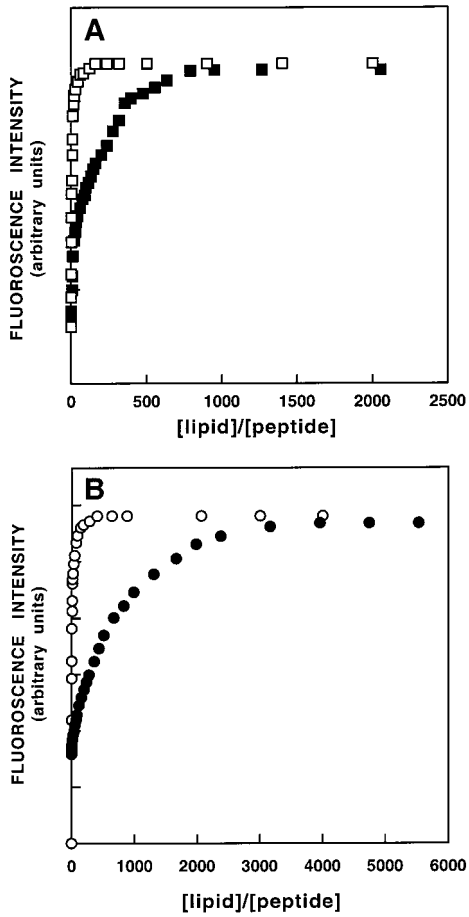

FIGURE 4: Panel A: Increases in the fluorescence of NBD-labeled linear melittin (□) and cyclic melittin (■) (0.1 μM total concentration) upon titration with PC/cholesterol vesicles, with the excitation wavelength set at 467 nm and emission at 530 nm. Details are as depicted in the legend to Figure 2. Panel B: Increases in the fluorescence of NBD-labeled linear magainin 2 analogue (○) and cyclic magainin 2 analogue (●) (0.1 μM total concentration) upon titration with PC/cholesterol.

that peptide cyclization, rather than the absence of MMTS blocking groups, lowers the affinity to PE/PG, PC/PG, and PC/cholesterol vesicles, the assay was repeated using the cyclic peptides under reducing conditions (2 mM DTT). The resulting unblocked and linearized peptides showed the same affinity to model membranes as their MMTS-blocked linear analogues.

Membrane Permeation Induced by the Peptides. To evaluate the effect of phospholipid membrane composition on peptide cell-selectivity, a membrane permeation study was performed. Various concentrations of the peptides were mixed with PE/PG or PC/cholesterol SUV, pretreated with the fluorescent dye diS-C_2-5 and valinomycin. Previous studies revealed that the effect of PE on membrane permeation is peptide-dependent. In the case of magainin, PE inhibited the magainin-induced pore formation (*58*), whereas an opposite effect was observed for 18L, a model cytolytic peptide (*59*), in which lytic activity increased with increasing content of PE (*60*). An additional factor that may influence peptide cytolytic activity is membrane curvature, which is high in SUV. To differentiate between contributions from lipid compostion and curvature, PC/PG (7:3 w/w) LUV were also investigated. Fluorescence recovery over time measured the kinetics of membrane disruption by peptides. We also determined the maximum recovery level as a function of the lipid to peptide molar ratio (Figure 5). The data reveal that all peptides significantly permeate PE/PG membranes (Figure 5A). Similar results were obtained in PC/PG LUV (Figure 5B). These results do not correlate with the large differences in antibacterial activity against *E. coli*, indicating that factors

Table 3: Partition Coefficient of the Peptides in the Presence of PE/PG (7:3, w/w), PC/PG (7:3, w/w), or PC/Cholesterol (10:1, w/w) Vesicles, As Determined by Nonlinear Least-Squares (NLLSQ) Fitting[a]

peptide designation	K_p* in PE/PG (M^{-1})	K_p* in PC/PG (M^{-1})	K_p* in PC/cholesterol (M^{-1})
linear melittin analogue	2.0 ($\pm$0.5) $\times$ 10^6	1.5 ($\pm$0.8) $\times$ 10^6	3.0 ($\pm$0.5) $\times$ 10^6
cyclic melittin analogue	5.1 ($\pm$0.6) $\times$ 10^5	3.7 ($\pm$0.7) $\times$ 10^5	1.0 ($\pm$0.5) $\times$ 10^5
linear magainin 2 analogue	2.7 ($\pm$0.5) $\times$ 10^6	1.1 ($\pm$0.3) $\times$ 10^6	1.5 ($\pm$0.5) $\times$ 10^6
cyclic magainin 2 analogue	3.1 ($\pm$0.6) $\times$ 10^5	0.9 ($\pm$0.4) $\times$ 10^5	2.2 ($\pm$0.4) $\times$ 10^4

[a] The results are the average of 3 independent repeats.

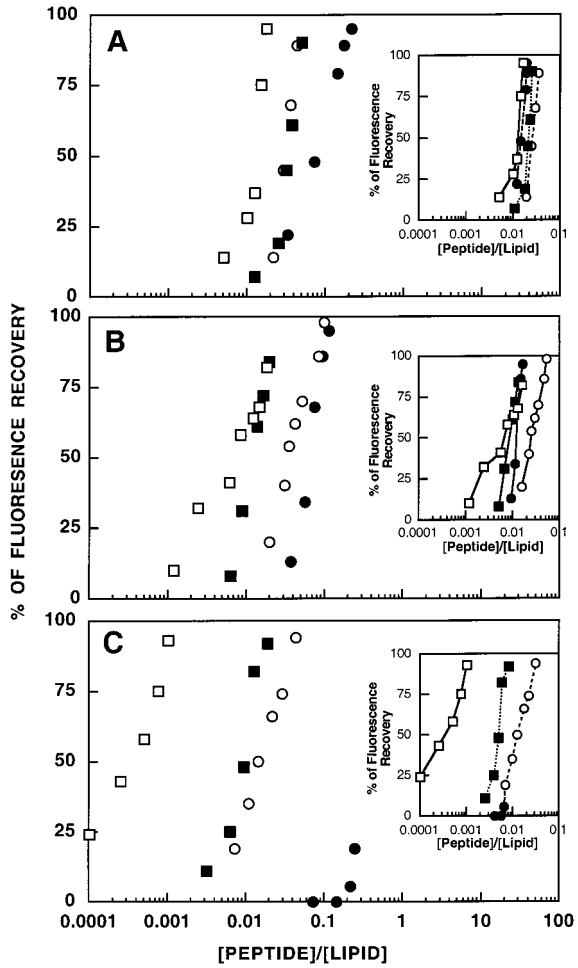

FIGURE 5: Maximal dissipation of the diffusion potential in vesicles induced by the peptides. The peptides were added to isotonic K^+-free buffer containing PE/PG SUV (panel A), PC/PG LUV (panel B), or PC/cholesterol SUV (panel C), preequilibrated with the fluorescent dye 3,3′-diethylthiodicarbocyanine iodide and valinomycin. Fluorescence recovery was measured 5−15 min after the peptides were mixed with the vesicles. Peptide designations: linear melittin (□); cyclic melittin (■); linear magainin 2 analogue (○); cyclic magainin 2 analogue (●).

other than peptide−lipid interactions are involved in the antibacterial activity of the peptides. In contrast, the results with zwitterionic membranes (Figure 5C) correlate well with the results of the hemolytic assay. Linear melittin is the most hemolytic and has the highest permeation activity on zwitterionic membranes. Cyclic magainin 2 analogue is the least hemolytic and has the lowest activity on PC/cholesterol.

To evaluate whether differences in the peptide's activities result from different amounts of bound peptides, the maximum fluorescence recovery as a function of the membrane-bound peptide to lipid molar ratio (determined from peptide binding curves) is plotted in the insets of Figure 5A−C. Linear and cyclic magainin analogues permeate PE/PG, PC/PG, and zwitterionic membranes similarly. However, linear and cyclic melittin only behave similarly with negatively charged PE/PG and PC/PG membranes.

To ensure that peptide cyclization, rather than the absence of the MMTS blocking groups, is responsible for the lower ability of the cyclic peptides to permeate PE/PG, PC/PG, and PC/cholesterol vesicles, the assay was repeated with the cyclic peptides in the presence of 2 mM DTT. Under reducing conditions, both cyclic melittin and cyclic magainin 2 had the same activity as their linear analogues without DTT. These results further reveal that blocking of the cysteine groups by MMTS does not affect the cytolytic activity of the peptides.

Table 4: Tryptophan Emission Maxima of the Peptides in Solution, in the Presence of PE/PG (7:3, w/w), or in PC/Cholesterol (10:1, w/w) Vesicles

peptide designation	PBS	PE/PG[a]	PC/cholesterol[a]
linear melittin analogue	349 ± 1	334 ± 1	336 ± 1
cyclic melittin analogue	348 ± 1	336 ± 1	341 ± 1
linear magainin 2 analogue	349 ± 1	337 ± 1	340 ± 1
cyclic magainin 2 analogue	348 ± 1	337 ± 1	341 ± 1

[a] A lipid to peptide molar ratio of 3000:1 was used in all cases. Under these conditions, more than 97% of the peptide is bound in all cases.

Characterization of the Environment of the Tryptophan Residue. To determine the environment of the peptides, we monitored the fluorescence emission spectrum of the tryptophan (*27*, *61*) in PBS at pH 7.4 or in the presence of vesicles composed of either PE/PG (7:3, w/w) or PC/cholesterol (10:1, w/w). Whereas disulfide bonds quench fluorescence, they have no effect on its blue shift (*62*). In these fluorometric studies, SUV were used to minimize light-scattering effects (*63*). A high lipid:peptide molar ratio was maintained (3000:1) so spectral contributions of free peptide would be negligible. The wavelength at the maximum intensity of the tryptophan emission was determined by fitting the emission spectra to log-normal distribution (*64*). Nonlinear least-squares (NLLSQ) analyses and data simulations were performed with the commercial software package Origin 6.0 (Microcal, Inc., Northampton MA). The results are summarized in Table 4. In buffer, the tryptophan residue of all four peptides is located in a hydrophilic environment (*27*). When PE/PG vesicles were added to the aqueous solutions containing the peptides, similar blue shifts were observed for all peptides reflecting their relocation to a more hydrophobic environment (*65*). In the presence of PC/cholesterol vesicles, only linear melittin exhibited a blue shift corresponding to a hydrophobic environment similar to that observed with PE/PG vesicles. All other peptides exhibited smaller blue shifts suggesting location in a more hydrophilic environment when in the presence of PC/cholesterol vesicles versus PE/PG vesicles.

The blue shift of the tryptophan emission of linear melittin can serve as a probe of peptide self-association in aqueous solution. Peptide oligomerization would cause shielding of the tryptophan in the largely hydrophobic interior of the oligomer from the aqueous medium (*66*, *67*). Linear melittin (0.1−40 μM) was added to PBS solution at pH 7.4, and the fluorescence emission spectrum of the tryptophan was monitored. The emission maximum of the tryptophan (349 ± 1 nm) was unchanged up to 15 μM peptide. Further increases in the concentration of linear melittin analogue resulted in a blue shift down to 345 ± 1 at 40 μM. This indicates that the peptide is predominantly monomeric at concentrations below 15 μM, and at higher concentrations it oligomerizes.

Secondary Structure of the Peptides Determined by CD Spectroscopy. The effect of cyclization on peptide secondary structure was assessed by CD spectroscopy recorded in PBS or in the presence of PE/PG SUV. Due to large light

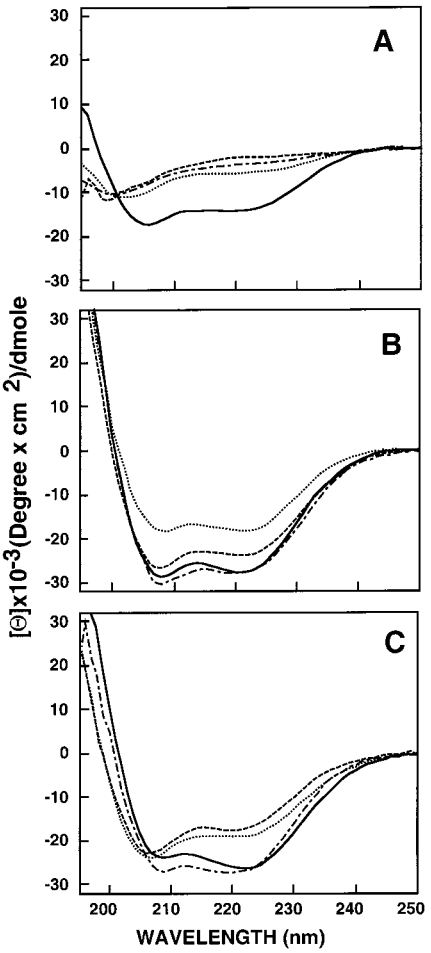

FIGURE 6: CD spectra of the peptides in PBS (panel A), in the presence of PE/PG SUV (panel B), or in 2% LPC micelles (panel C). Spectra were taken at peptide concentrations of 1.5×10^{-5} to 2.0×10^{-5} M. The assay was performed as described under Materials and Methods. Linear melittin (—); cyclic melittin (···); linear magainin 2 analogue (— · —); cyclic magainin 2 analogue (- - -).

scattering effects of PC/cholesterol SUV, the CD spectra of the peptides in the presence of zwitterionic membranes were studied using 2% lysophosphatidylcholine (LPC) micelles. The CD spectral profiles of peptides in PBS, PE/PG SUV, and LPC micelles are shown in Figures 6A, 6B, and 6C, respectively. The lipid:peptide molar ratios used were 325:1 in the case of PE/PG and 2100:1 in the case of LPC. Assuming that partitioning to LPC is similar to PC, the binding experiments suggest that >96% of melittin and cyclic melittin is bound to PE/PG and LPC. In the case of magainin, >96% of the linear form is bound to PE/PG and LPC, while ~75% and ~79% of the cyclic form are bound to PE/PG and LPC, respectively. The mean residual ellipticities, $[\theta]_{222}$, and the corresponding percentages of α-helix of the peptides are summarized in Table 5. The numbers in parentheses are the actual values after corrections for the fraction bound. In buffer, only linear melittin adopted significant α-helical structure, most probably from aggregation due to hydrophobic interactions, as was also observed in the tryptophan blue shift experiment described above. Interestingly, cyclization did not have a strong effect on the structure of melittin and magainin 2 analogues. Both peptides preserved most of their α-helical structure.

DISCUSSION

Melittin and magainin 2 are thought to bind and insert into membranes by (i) interfacial binding of the unfolded peptide, due mainly to electrostatic interactions in the case of magainin 2 (*68*, *69*), or hydrophobic interactions in the case of melittin (*70*); (ii) insertion of the nonpolar side chains into the hydrophobic core of the membrane; and (iii) transition from a random coil to an α-helical structure coupled with insertion into the lipid bilayers (*69*, *71*). It should be noted that analogues of magainin 2 and melittin were used in this study. These analogues are different from those reported for magainin (*72*) and melittin (*32*), and, therefore, their binding constants are different. These differences can be explained by taking into account the substitutions made to the peptides, the effect of positive charge to the binding constant (*73*), and the contribution of the added and substituted amino acids to the binding of the peptides to phospholipid membranes (*74*).

Cyclization Allows Differentiation between Contributions from Random Coil to α-Helix Transitions and Electrostatic Interactions Involved in Magainin 2 Membrane Binding. The binding study (Figures 2−4 and Table 3) reveals that linear magainin 2 analogue has a similar affinity toward net negatively charged membranes and zwitterionic phospholipid membranes. This indicates the large contribution of random coil to α-helix transition to the membrane binding ability of the peptide, as compared to electrostatic attraction. These results are further supported by a recent thermodynamic study showing that helix formation accounts for about 50% of the free energy of binding of magainin 2 to lipid bilayers (*69*). Indeed, cyclization of magainin 2 analogue reduced its helical structure in zwitterionic phospholipid membranes and there-

Table 5: Mean Residual Ellipticity at 222 nm ($[\theta]_{222}$) and Derived α-Helical Content of the Peptides in PBS, in the Presence of PE/PG (7:3 w/w) SUV, or in 2% LPC Micelles[a]

	PBS		PE/PG[b]		LPC[c]	
peptide designation	$[\theta]_{222}$ [d]	% α-helix	$[\theta]_{222}$	% α-helix	$[\theta]_{222}$	% α-helix
linear melittin analogue	−13970	40	−25100	77	−26600	82
cyclic melittin analogue	−5460	11	−19080	57	−23000	70
linear magainin 2 analogue	−3400	5	−26580	82	−27600	85
cyclic magainin 2 analogue	−2020	0	−15800	46	−16400	48
			(−21100)	(64)	(−21100)	(64)

[a] Standard error is ±4%. [b] A peptide to lipid molar ratio of 1:325 was used, in which >96% of the peptides (besides cyclic magainin that binds only ~75%) are bound to the PE/PG SUV as revealed by their binding curves (Figure 2). Numbers in parentheses are after correction for bound peptide. [c] A peptide to LPC molar ratio of 2100:1 was used in which ~100% of the peptides (besides cyclic magainin that binds only ~78%) are bound to the LPC as revealed by their binding curves (Figure 4) and assuming partitioning similar to PC. Numbers in parentheses are after correction for bound peptide. [d] $[\theta]_{222}$ in deg·cm²/dmol.

fore interfered with the coil to α-helix transition. The result is a significant reduction in its affinity to these membranes (~70-fold). Even more interestingly, cyclization brought forward the contribution of electrostatic interactions: Table 3 shows that cyclic magainin 2 analogue has about an order of magnitude preference for negatively charged over PC/cholesterol phospholipid membranes. However, cyclic magainin 2 analogue adopts the same amount of α-helical structure (Table 5) and possesses similar membrane-permeating activity [after correction for the amount of peptide bound (insets of Figure 5A−C)] in both zwitterionic and negatively charged phospholipid membranes. This indicates that the large difference in affinity results from electrostatic attraction to the surface of net negatively charged membranes, and repulsion in the case of the positively charged choline headgroups.

Melittin Approaches the Membrane with Its Hydrophobic Regions followed by Its Positively Charged Region. In addition to electrostatic interactions and a coil−helix transition, the role of hydrophobicity in the binding and insertion of melittin analogues is more predominant compared to magainin analogues. This is demonstrated in the following data: (i) Despite the fact that melittin analogue has +6 net charge and magainin analogue +5, cylization caused only a 4-fold decrease in melittin binding to negatively charged membraes compared to a ~10-fold decrease in magainin. Furthermore, with PC membranes, cyclization caused a ~30-fold decrease in melittin binding compared to ~70-fold in magainin analogue. (ii) Cyclic melittin has a ~4−5-fold decrease in affinity toward PC compared to negatively charged membranes, whereas cyclic magainin has a ~18-fold decrease. A possible explanation for the strong reduction in the affinity of cyclic melittin to PC compared to the linear form is as follows: The sequence of molecular events involved in the interaction of melittin with membranes was studied using fluorescence techniques (*70*). The hydrophobic regions of melittin rapidly bind and insert into the membrane followed by its positively charged terminus. Attaching the hydrophobic and positively charged regions of the molecule together by disulfide bonds seems to interrupt with this sequence of events, and interfere with the initial membrane interaction of the hydrophobic regions. Thus, the higher affinity of the cyclic melittin to negatively charged membranes, as compared to zwitterionic membranes, may result from the involvement of the positively charged region of the molecule in initial membrane interactions.

The Role of Linearity on the Activity of Magainin and Melittin Analogues. Cyclization of magainin 2 analogue significantly reduces cytolytic activity toward both erythrocytes (Figure 1) and bacteria (Table 2). Contrary to magainin, cyclization of melittin analogue significantly reduces its hemolytic activity but preserves or increases activity toward bacteria. The reduction in hemolytic activity of both peptides upon cyclization (Figure 1) correlates with a reduction in their binding (Table 3) and permeating activity toward PC/cholesterol membranes (Figure 5C), the major component of the outer leaflet of red blood cells (*57*). The reduction may be more pronounced with cyclic magainin analogue because its helical structure is altered more than cyclic melittin, and its binding is highly driven by electrostatic interactions and a random coil−helix transition (see previous paragraphs). Interestingly, at similar bound peptide:lipid molar ratios, both linear and cyclic magainin analogues have similar membrane permeation activity with both types of phospholipids (insets of Figure 5A−C), indicating that linearity is not required for membrane permeation. This points to the role of linearity in reaching the target bacterial membrane. To reach the target bacterial phospholipid membrane, peptides must cross several barriers, such as lipopolysaccharides and peptidoglycan of Gram-negative bacteria or polysaccharides (teichoic acids) in Gram-positive bacteria. Our results indicate that it is more difficult for the cyclic magainin analogue than for the cyclic melittin analogue to cross these barriers. A major difference between magainin and melittin analogues resides in the pattern of amino acid distribution. The 22 amino acid N-terminal of the melittin analogue is highly hydrophobic and is followed by 4 consecutive positively charged residues and 2 glutamines. Upon cyclization, all the charges, including the N-terminal free amine, remain on a small portion of the ring and most of the ring is hydrophobic. In contrast, the five positively charged amino acids in magainin are distributed along its amphipatic helix. Upon cyclization, all the positive charges, including the N-terminal free amine, are distributed throughout the ring, and the peptide becomes less helical (Table 5). These changes can cause more efficient binding of cyclic magainin analogue to the negatively charged cell wall components, and hence make it more difficult for the cyclic form to diffuse to the inner target phospholipid membrane.

The differences between the activity of the linear versus cyclic versions of the peptides are more pronounced with *E. coli*. Contrary to the magainin analogue, while cyclic melittin was more active than the linear peptide toward *E. coli*, the opposite results were observed in the membrane permeation study. These results point to yet another factor that may be involved in the cytolytic activity of the peptides. This factor is self-association of linear melittin in solution as compared to its cyclic form. Linear melittin, but not its cyclic form, oligomerizes at concentrations higher than 15 μM as revealed by CD experiments in buffer (Figure 6A) and Trp fluorescence studies. Thus, linear melittin may bind *E. coli* membrane as an oligomer (the MIC is 30 μM), whereas its cyclic form binds as monomers. The lower activity of the linear form may simply be related to its more difficult diffusion through the outer surface of Gram-negative bacteria. It should be noted that decyclization of some cyclic peptides forming predominantly β-sheet stuctures also severely decreases their antimicrobial activity. Examples include tachypelsin I (*75*) and gramicidin S (*76*). Since Gram-positive bacteria contain only one membrane, such differences are less significant.

Previous studies revealed that magainin 2 induces transient holes in phospholipid membranes. A torodial (or wormhole) model for pore formation was suggested, in which the lipid bends back on itself like the inside of a torus (*77*−*79*). Linear peptide monomers act as fillers in the expansion region, thereby stabilizing the pore. When a pore is closed, the participating peptide monomers will again adsorb onto the headgroup region, but they may surface to either side of the membrane (*77*). The membrane permeation study reveals that the linearity of the magainin 2 analogue is not essential for phospholipid membrane disruption (Figure 5A), and therefore agrees with the notion that the magainin analogue probably does not form an organized pore but has a detergent-like

effect, as described in the carpet model [reviewed in (*41*, *42*)]. It should be noted that the step prior to membrane miscellization also includes transient holes [step 2 in the carpet model (*42*)].

In summary, our results indicate that the linearity of magainin 2 and melittin is not essential for the disruption of the target phospholipid membrane, but rather provides the means to reach it. In the case of magainin 2, linearity may enable the peptide to cross the outer bacterial layers composed of LPS and peptidoglycan or polysaccharides, while in the case of melittin linearity allows it to manifest its hydrophobicity, and to nonselectively interact and lyse a variety of phospholipid membranes. Importantly, the results of the present study demonstrate the utility of the cyclic peptide analogue approach to examine the driving forces for membrane partitioning of amphipathic α-helical peptides. Disruption of the coil−helix transition of the peptides, while maintaining the same sequence of hydrophobic and positively charged amino acids, allowed separate examination of the contribution of hydrophobic and electrostatic interactions to membrane binding of these peptides. These results should also assist in the development of potent and selective antimicrobial peptides.

REFERENCES

1. Epand, R. M. (1993) *The Amphipathic Helix*, CRC Press, Boca Raton, FL.
2. White, S. H., and Wimley, W. C. (1999) *Annu. Rev. Biophys. Biomol. Struct. 28*, 319−365.
3. Habermann, E., and Jentsch, J. (1967) *Hoppe-Seyler's Z. Physiol. Chem. 348*, 37−50.
4. Zasloff, M. (1987) *Proc. Natl. Acad. Sci. U.S.A. 84*, 5449−5453.
5. Talbot, J. C., Dufourcq, J., de Bony, J., Faucon, J. F., and Lussan, C. (1979) *FEBS Lett. 102*, 191−193.
6. Lauterwein, J., Brown, L. R., and Wuthrich, K. (1980) *Biochim. Biophys. Acta 622*, 219−230.
7. Brown, L. R., and Wuthrich, K. (1981) *Biochim. Biophys. Acta 647*, 95−111.
8. Brown, L. R., Braun, W., Kumar, A., and Wuthrich, K. (1982) *Biophys. J. 37*, 319−328.
9. Inagaki, F., Shimada, I., Kawaguchi, K., Hirano, M., Terasawa, I., Ikura, T., and Go, N. (1989) *Biochemitry 28*, 5985−5991.
10. Okada, A., Wakamatsu, K., Miyazawa, T., and Higashijima, T. (1994) *Biochemistry 33*, 9438−9446.
11. Altenbach, C., Froncisz, W., Hyde, J. S., and Hubbell, W. L. (1989) *Biophys. J. 56*, 1183−1191.
12. Frey, S., and Tamm, L. K. (1991) *Biophys. J. 60*, 922−930.
13. Kleinschmidt, J. H., Mahaney, J. E., Thomas, D. D., and Marsh, D. (1997) *Biophys. J. 72*, 767−778.
14. Wieprecht, T., Dathe, M., Schumann, M., Krause, E., Beyermann, M., and Bienert, M. (1996) *Biochemistry 35*, 10844−10853.
15. Duclohier, H., Molle, G., and Spach, G. (1989) *Biophys. J. 56*, 1017−1021.
16. Matsuzaki, K., Harada, M., Handa, T., Funakoshi, S., Fujii, N., Yajima, H., and Miyajima, K. (1989) *Biochim. Biophys. Acta 981*, 130−134.
17. Bechinger, B., Zasloff, M., and Opella, S. J. (1993) *Protein Sci. 2*, 2077−2084.
18. Gesell, J., Zasloff, M., and Opella, S. J. (1997) *J. Biomol. NMR 9*, 127−135.
19. Bechinger, B., Kim, Y., Chirlian, L. E., Gesell, J., Neumann, J. M., Montal, M., Tomich, J., Zasloff, M., and Opella, S. J. (1991) *J. Biomol. NMR 1*, 167−173.
20. Hirsh, D. J., Hammer, J., Maloy, W. L., Blazyk, J., and Schaefer, J. (1996) *Biochemistry 35*, 12733−12741.
21. Williams, R. W., Starman, R., Taylor, K. M., Gable, K., Beeler, T., Zasloff, M., and Covell, D. (1990) *Biochemistry 29*, 4490−4496.
22. Matsuzaki, K., Murase, O., Tokuda, H., Funakoshi, S., Fujii, N., and Miyajima, K. (1994) *Biochemistry 33*, 3342−3349.
23. Steiner, H., Hultmark, D., Engstrom, A., Bennich, H., and Boman, H. G. (1981) *Nature 292*, 246−248.
24. Blondelle, S. E., and Houghten, R. A. (1991) *Biochemistry 30*, 4671−4678.
25. Habermann, E. (1972) *Science 177*, 314−322.
26. Hider, R. C., Khader, F., and Tatham, A. S. (1983) *Biochim. Biophys. Acta 728*, 206−214.
27. Dufourcq, J., and Faucon, J. F. (1977) *Biochim. Biophys. Acta 467*, 1−11.
28. Batenburg, A. M., van, E. J., Leunissen, B. J., Verkleij, A. J., and de Kruijff, B. (1987) *FEBS Lett. 223*, 148−154.
29. Batenburg, A. M., Hibbeln, J. C., and de Kruijff, B. (1987) *Biochim. Biophys. Acta 903*, 155−165.
30. Batenburg, A. M., Hibbeln, J. C., Verkleij, A. J., and de Kruijff, B. (1987) *Biochim. Biophys. Acta 903*, 142−154.
31. Batenburg, A. M., van, E. J., and de Kruijff, B. (1988) *Biochemistry 27*, 2324−2331.
32. Beschiaschvili, G., and Seelig, J. (1990) *Biochemistry 29*, 52−58.
33. Gomes, A. V., De Waal, A., Berden, J. A., and Westerhoff, H. V. (1993) *Biochemistry 32*, 5365−5372.
34. Matsuzaki, K., Sugishita, K., Fujii, N., and Miyajima, K. (1995) *Biochemistry 34*, 3423−3429.
35. Batenburg, A. M., and de Kruijff, B. (1988) *Biosci. Rep. 8*, 299−307.
36. DeGrado, W. F., Musso, G. F., Lieber, M., Kaiser, E. T., and Kezdy, F. J. (1982) *Biophys. J. 37*, 329−338.
37. Vogel, H., and Jahnig, F. (1986) *Biophys. J. 50*, 573−582.
38. Cruciani, R. A., Barker, J. L., Zasloff, M., Chen, H. C., and Colamonici, O. (1991) *Proc. Natl. Acad. Sci. U.S.A. 88*, 3792−3796.
39. Matsuzaki, K., Harada, M., Funakoshi, S., Fujii, N., and Miyajima, K. (1991) *Biochim. Biophys. Acta 1063*, 162−170.
40. Dempsey, C. E. (1990) *Biochim. Biophys. Acta 1031*, 143−161.
41. Matsuzaki, K. (1999) *Biochim. Biophys. Acta 1462*, 1−10.
42. Oren, Z., and Shai, Y. (1998) *Biopolymers 47*, 451−463.
43. Rapaport, D., and Shai, Y. (1991) *J. Biol. Chem. 266*, 23769−23775.
44. Papahadjopoulos, D., and Miller, N. (1967) *Biochim. Biophys. Acta 135*, 624−638.
45. Sims, P. J., Waggoner, A. S., Wang, C. H., and Hoffmann, J. R. (1974) *Biochemistry 13*, 3315−3330.
46. Loew, L. M., Rosenberg, I., Bridge, M., and Gitler, C. (1983) *Biochemistry 22*, 837−844.
47. Shai, Y., Bach, D., and Yanovsky, A. (1990) *J. Biol. Chem. 265*, 20202−20209.
48. Greenfield, N., and Fasman, G. D. (1969) *Biochemistry 8*, 4108−4116.
49. Wu, C. S., Ikeda, K., and Yang, J. T. (1981) *Biochemistry 20*, 566−570.
50. Schumann, M., Dathe, M., Wieprecht, T., Beyermann, M., and Bienert, M. (1997) *Biochemistry 36*, 4345−4351.
51. Cuvero, J. H., Rodriguez, B., and Houghten, R. A. (1990) in *Peptides-Chemistry and Biology* (Rivier, J. E. and Marshall, G. R., Eds.) pp 124−126, ESCOM, Leiden.
52. Gazit, E., and Shai, Y. (1993) *Biochemistry 32*, 3429−3436.
53. Oren, Z., Lerman, J. C., Gudmundsson, G. H., Agerberth, B., and Shai, Y. (1999) *Biochem. J. 341*, 501−513.
54. Chan, T., and Shellenberg, K. (1968) *J. Biol. Chem. 243*, 6284−6289.
55. Cowgill, R. W. (1967) *Biochim. Biophys. Acta 140*, 37−38.
56. Shaw, N. (1974) *Adv. Appl. Microbiol. 17*, 63−108.
57. Verkleij, A. J., Zwaal, R. F., Roelofsen, B., Comfurius, P., Kastelijn, D., and Deenen, L. V. (1973) *Biochim. Biophys. Acta 323*, 178−193.
58. Matsuzaki, K., Sugishita, K., Ishibe, N., Ueha, M., Nakata, S., Miyajima, K., and Epand, R. M. (1998) *Biochemistry 37*, 11856−11863.

59. Tyler, M. E., Segrest, J. P., Epand, R. M., Nie, S. Q., Epand, R. F., Mishra, V. K., Venkatachalapathi, Y. V., and Anantharamaih, G. M. (1993) *J. Biol. Chem. 29*, 22112−22118.
60. Polozov, I. V., Polozova, A. I., Tytler, E. M., Anantharamaiah, G. M., Segrest, J. P., Woolley, G. A., and Epand, R. M. (1997) *Biochemistry 36*, 9237−9245.
61. Vogel, H. (1981) *FEBS Lett. 134*, 37−42.
62. Oren, Z., and Shai, Y. (2000) *Biochemistry 39*, 6103−6114.
63. Mao, D., and Wallace, B. A. (1984) *Biochemistry 23*, 2667−2673.
64. Ladokhin, A. S., Jayasinghe, S., and White, S. H. (2000) *Anal. Biochem. 285*, 235−245.
65. Talbot, J. C., Faucon, J. F., and Dufourcq, J. (1987) *Eur. Biophys. J. 15*, 147−157.
66. Terwilliger, T. C., and Eisenberg, D. (1982) *J. Biol. Chem. 257*, 6016−6022.
67. Veen, M. V., Georgiou, G. M., Drake, A. F., and Cherry, R. J. (1995) *Biochem. J. 305*, 785−790.
68. Wieprecht, T., Beyermann, M., and Seelig, J. (1999) *Biochemistry 38*, 10377−10387.
69. Wieprecht, T., Apostolov, O., Beyermann, M., and Joachim, S. (1999) *J. Mol. Biol. 294*, 785−794.
70. Wolfe, C., Cladera, J., and O'Shea, P. (1998) *Mol. Membr. Biol. 15*, 221−227.
71. Ladokhin, A. S., and White, S. H. (1999) *J. Mol. Biol. 285*, 1363−1369.
72. Wenk, M. R., and Seelig, J. (1998) *Biochemistry 37*, 3909−3916.
73. Murray, D., Arbuzova, A., Hangyas-Mihalyne, G., Gambhir, A., Ben-Tal, N., Honig, B., and McLaughlin, S. (1999) *Biophys. J. 77*, 3176−3188.
74. White, S. H., and Wimley, W. C. (1998) *Biochim. Biophys. Acta 1376*, 339−352.
75. Tamamura, H., Ikoma, R., Niwa, M., Funakoshi, S., Murakami, T., and Fujii, N. (1993) *Chem. Pharm. Bull. (Tokyo) 41*, 978−980.
76. Kondejewski, L. H., Farmer, S. W., Wishart, D. S., Hancock, R. E., and Hodges, R. S. (1996) *Int. J. Pept. Protein Res. 47*, 460−466.
77. Matsuzaki, K., Murase, O., Fujii, N., and Miyajima, K. (1995) *Biochemistry 34*, 6521−6526.
78. Ludtke, S. J., He, K., Heller, W. T., Harroun, T. A., Yang, L., and Huang, H. W. (1996) *Biochemistry 35*, 13723−13728.
79. Matsuzaki, K., Murase, O., Fujii, N., and Miyajima, K. (1996) *Biochemistry 35*, 11361−11368.

BI0026066